Electronic Supplementary Material (ESI) for Dalton Transactions.
This journal is © The Royal Society of Chemistry 2021

Supplementary Information

Compressive and Thermally Stable Boron Nitride Aerogel as Multifunctional Sorbent

Dong Xia[a, f], Huayang Yu[b, f], Qun Li[c], Jamie Mannering[a], Robert Menzel[a], Peng Huang[d]* and Heng Li[e]*

[a] School of Chemistry, University of Leeds, Leeds, LS2 9JT, UK
[b] School of Design, University of Leeds, Leeds, LS2 9JT, UK
[c] Department of Chemical and Biochemical Engineering, College of Chemistry and Chemical Engineering, Xiamen University, Xiamen 361005, China
[d] Department of Materials, University of Manchester, Manchester, M13 9PL, UK
[e] Key Laboratory of Estuarine Ecological Security and Environmental Health, Tan Kah Kee College, Xiamen University, 363105, Zhangzhou, China
[f] These authors contributed equally: Dong Xia, Huayang Yu.

*Corresponding author: Dr Peng Huang, Email: peng.huang@manchester.ac.uk;
Dr Heng Li, Email: liheng@xujc.com

Experimental section

Materials: Boric acid, melamine, dibenzothiophene (DBT) and commercial boron nitride (BN) powder were obtained from Sigma-Aldrich (UK). HPLC water, dioxane, n-octane and hexane were supplied by Fisher Scientific (UK). All chemicals were used as received.

Synthesis of BN aerogels: Boric acid (a fixed amount of 0.3156 g was used) and melamine with different mole ratios (2:0.5, 2:1, 2:2, 2:2.5, 2:3) were dissolved in a solution of water/dioxane (v/v = 2:1) at 85 ^{o}C, with vigorous stirring, until the formation of a uniform mixture. After which, the mixture was transferred into a customised mold (or 15 mL centrifuge tubes) and cooled down to ambient temperature to form hydrogels. Then, the hydrogel-contained mold was immersed in liquid nitrogen, followed by freeze-drying for 48 h to obtain the white aerogel precursor. The aerogel precursor was subsequently annealed in a tube furnace at 1000 ^{o}C for 2 h in an H_2/N_2 (5% H_2) atmosphere. After cooling down to ambient temperature, the final BN aerogel was obtained as a white solid and stored for subsequent use. According to the nominal mole ratios of the starting materials, the aerogels were designated as BN(2:3) aerogel, BN(2:6) aerogel, BN(2:12) aerogel, BN(2:15) aerogel and BN(2:18) aerogel, respectively.

Materials characterisation: Powder X-ray diffraction (XRD) patterns were collected on a Bruker D2 Phaser Diffractometer using Cu K_α radiation. Scanning electron microscopic analyses (SEM) were conducted on a Nova NanoSEM 450 with an accelerating voltage of 3 keV. Specimens were fixed onto aluminium stubs using conductive carbon tapes without coating. Raman spectra of the BN aerogels were collected using a Renishaw InVia Raman microscope with an excitation laser wavelength of 532 nm, between 400 and 4000 cm^{-1}. Infrared spectroscopic analyses (IR) were performed on a PerkinElmer Spectrum One FT-IR spectrometer, with a scanning range from 550 to 4000 cm^{-1}. Brunauer-Emmett-Teller (BET) nitrogen adsorption/desorption isotherms were acquired using a Micromeritics TriStar 3000 instrument. The aerogel samples were degassed under N_2 gas at 110 ^{o}C for 3 hours prior to analysis. Nitrogen adsorption and desorption isotherms were measured at 77 K. The pore diameter distribution of the samples was calculated from the desorption isotherm using the Barrett-Joyner-Halenda (BJH) method. The compression stress-strain curves were measured using an Instron 5566 model mechanical testing machine at a loading speed of 5 mm/min. Thermogravimetric analysis (TGA) was performed on a PerkinElmer Pyris One instrument, under an air atmosphere. The samples were heated from ambient temperature to 900 °C, at a heating rate of 10 °C/min. Transmission electron microscopy (TEM) images were collected from an electron microscope (Tecnai F30, FEI) at an accelerating voltage of 300 kV. X-ray photoelectron spectroscopy (XPS) spectrum was measured on a K-Alpha^{+} X-ray photoelectron spectrometer (Thermo Fisher Scientific), using focused (400 μm spot size) monochromatic Al-Kα radiation. All the binding energies were referenced to the C1s peak of adventitious carbon at 284.8 eV.

Bragg's law and Scherrer equation: The lattice spacing (d) was calculated from the XRD peaks (here 002 peak in the XRD patterns) using Bragg's law (Eq. 1). Then, the average crystallite domain size (D_p) of the BN aerogels were calculated from the same XRD diffraction peaks, using the Scherrer equation (Eq. 2). When dividing the (002) crystallite domain size, D_{002} (i.e. the crystallite size in the direction of the BN sheets stacking), by the basal plane spacing of the BN sheet, d_{002}, the number of BN sheets in the crystallite domain, i.e. the average number of sheets stacked with high crystalline order, can be estimated (layer number = $D_p/d + 1$).

Bragg's law and Scherrer equation: The lattice spacing was determined by Bragg's law using the equation below:

$$2d \cdot sin\theta = n \cdot \lambda \qquad \textit{Eq. 1}$$

Where d is the lattice spacing (nm), θ is the diffraction angle, λ is the X-ray wavelength (0.154178 nm), and n is an integer.

The mean crystallite domain size of the aerogels was calculated using the full-width at half-maximum (FWHM) of the (002) peak. The equation is as follows:

$$D_p = \frac{k \cdot \lambda}{\beta \cdot cos\theta} \qquad \textit{Eq. 2}$$

Where D_p is the mean crystallite domain size (nm) along the (002) direction, k is a dimensionless shape factor (0.94), β is the FWHM of the peak, and θ is the diffraction angle.

Oil absorption/desorption: The BN aerogel was placed in n-octane solution (oil) until equilibrium was reached. Afterwards, the aerogel was taken out from the solution using a tweezer. The desorption of the oil was performed by squeezing the aerogel by hand.

Adsorptive desulfurization measurements: BN aerogel (20 mg) was added to a DBT-contained (initial DBT concentration of 500 ppm sulfur, 500 ppm·S) n-octane solution (10 mL) and stirred at 20 °C for 3 h. Each measurement was accompanied by a pure DBT reference solution for the subsequent quantification of adsorbed DBT. To determine DBT uptake capacity, the adsorbent/fuel mixtures were centrifuged to remove particles before being measured by gas chromatography (GC, Agilent 7890B GC system with an HP-5 column). All experiments were performed in triplicate and presented using the average values. The removal of adsorbed DBT molecules on BN aerogels were conducted in a tube furnace at 400 ^{o}C under a nitrogen atmosphere.

CO_2 adsorption measurements: The CO_2 adsorption isotherm was measured on a Quantachrome Autosorb iQ gas adsorption instrument. The BN aerogels were degassed before CO_2 adsorption measurements. The temperature of the adsorption experiment was controlled by a heating circulator.

Results and discussion

Fig. S1 Digital photo of customized molds for the preparation of BN aerogels.

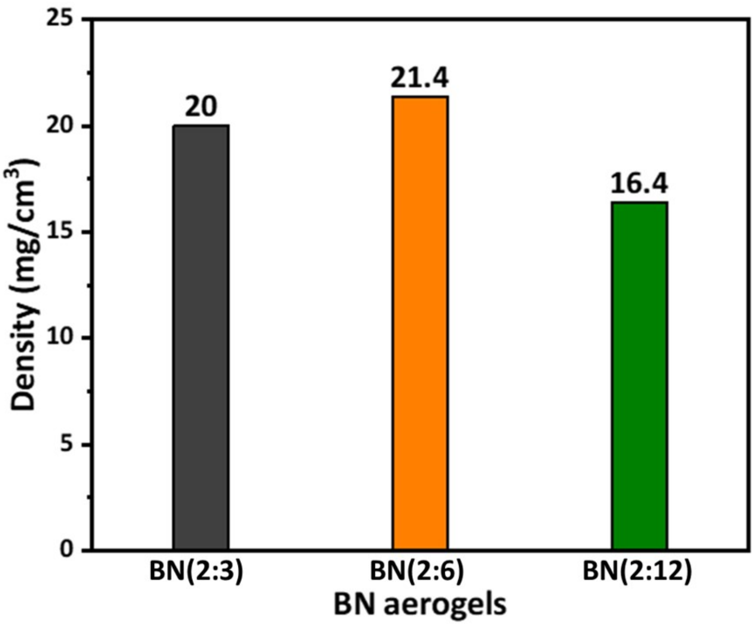

Fig. S2 Density of different BN aerogels.

Fig. S3 A digital photo of a BN aerogel prepared in a centrifuge tube.

Table S1. Physical properties of the prepared BN aerogels

Sample	D_p (nm)	*d* (nm)	*Number of layers (n)*
BN(2:3) aerogel	1.29	0.35	5
BN(2:6) aerogel	1.32	0.35	5
BN(2:12) aerogel	0.79	0.36	3
BN(2:15) aerogel	1.28	0.35	5
BN(2:18) aerogel	1.16	0.35	4

[a] D_p, mean crystallite domain size, as calculated from the (002) plane; *d*, lattice spacing.

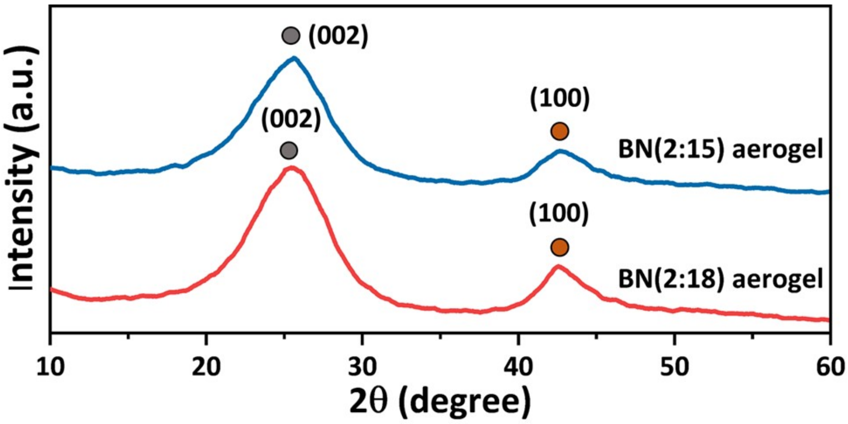

Fig. S4 XRD patterns of BN(2:15) aerogel and BN(2:18) aerogel.

Fig. S4 exhibits two diffraction peaks attributing to typical (002) and (100) plane of BN aerogels, with the BN(2:15) aerogel and BN(2:18) aerogel showing 5 and 4 layers of BN nanosheets (Table S1), respectively.

Table S2. Parameters of the BN aerogels from Raman analyses

Sample	*Peak position of* E_{2g} (cm^{-1})	*FWHM* (cm^{-1})
BN(2:3) aerogel	1410	841
BN(2:6) aerogel	1369	738
BN(2:12) aerogel	1371	770

Table S3. Specific surface area and pore volume accumulation of the BN aerogels.

Sample	*Specific surface area (m²/g)*	*V_{pore} (cm³/g)*
BN(2:3) aerogel	280	0.065
BN(2:6) aerogel	938	0.190
BN(2:12) aerogel	651	0.251

Table S4. Atomic ratios of C, O, B and N elements in different BN aerogels

Sample	C (atomic %)	O (atomic %)	B (atomic %)	N (atomic %)	B/N ratio	B lost (%)
BN(2:3) aerogel precursor	31.2	28.8	19.2	20.8	0.95	--
BN(2:6) aerogel precursor	31.5	25.5	16.4	26.6	0.62	--
BN(2:12) aerogel precursor	35.9	15.5	8.2	40.3	0.20	--
BN(2:3) aerogel	8.0	13.5	46.8	31.7	1.48	46
BN(2:6) aerogel	8.7	13.5	45.7	32.1	1.42	43
BN(2:12) aerogel	9.0	12.7	41.4	36.9	1.12	26

The percentage of C/O elements were 8.0%/13.5%, 8.7%/13.5% and 9.0%/12.7% in the BN(2:3) aerogel, BN(2:6) aerogel and BN(2:12) aerogel, respectively. The B/N ratio is significantly increased after the thermal annealing treatment, owing to the release of melamine. Specifically, the B/N ratio in the BN(2:3) aerogel, BN(2:6) aerogel and BN(2:12) aerogel is 1.48, 1.42 and 1.12, respectively. The percentage of B lost during freeze-drying and thermal annealing was 46%, 43%, and 26% in the BN(2:3) aerogel, BN(2:6) aerogel, and BN(2:12) aerogel (Table S4), respectively.

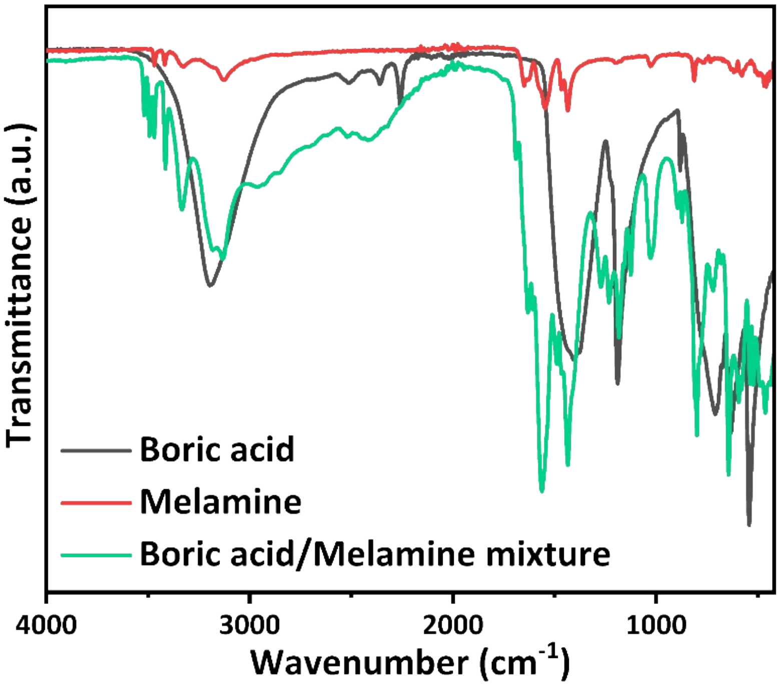

Fig. S5 FT-IR spectra of boric acid, melamine, and boric acid/melamine mixture.

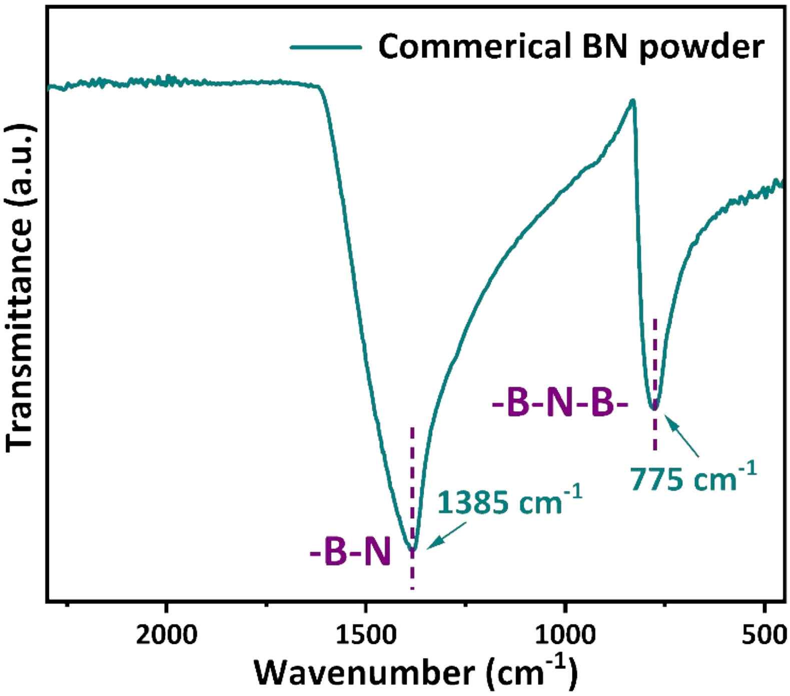

Fig. S6 FT-IR spectrum of commercial BN powder.

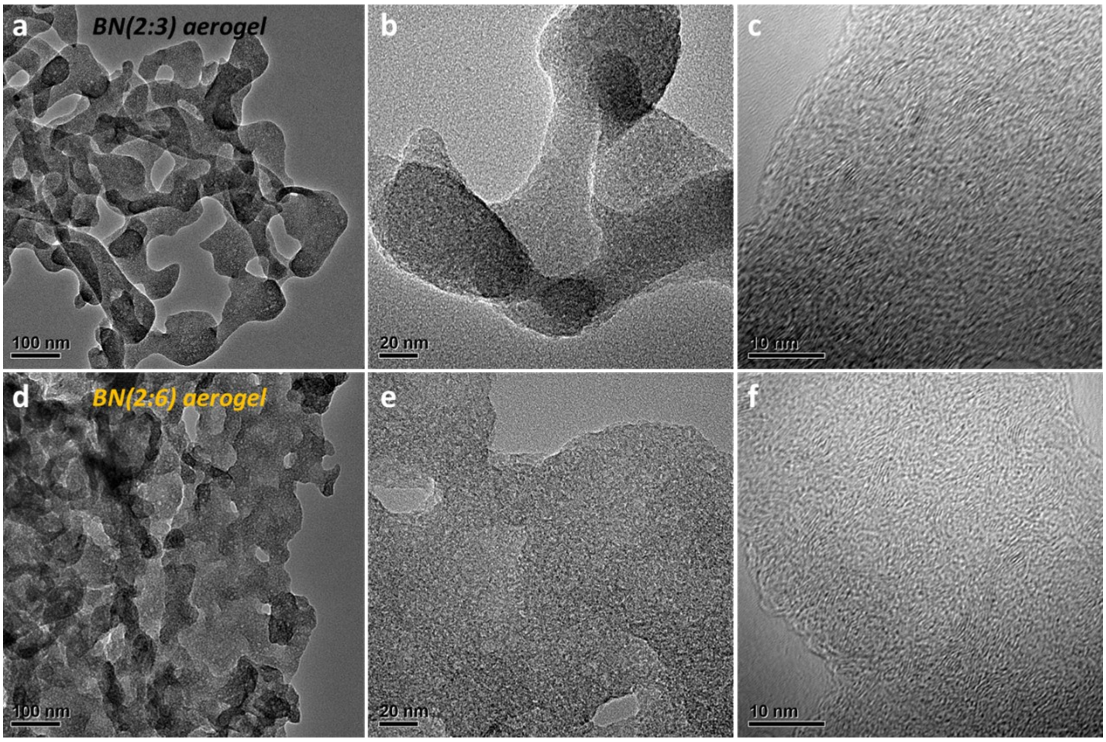

Fig. S7 TEM images of BN(2:3) aerogel (a-c) and BN(2:6) aerogel (d-f) with different magnifications.

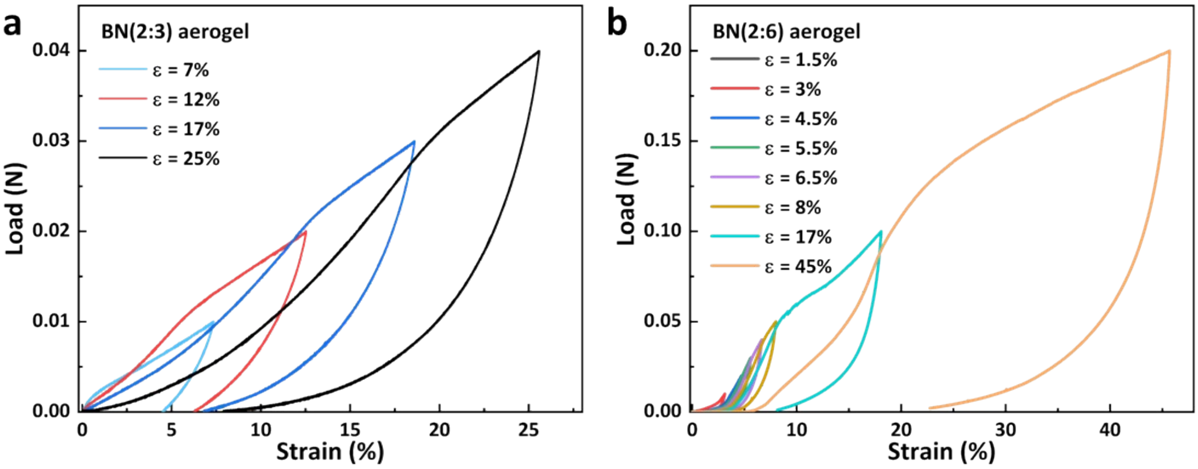

Fig. S8 Load-strain curves of BN(2:3) aerogel and BN(2:6) aerogel.

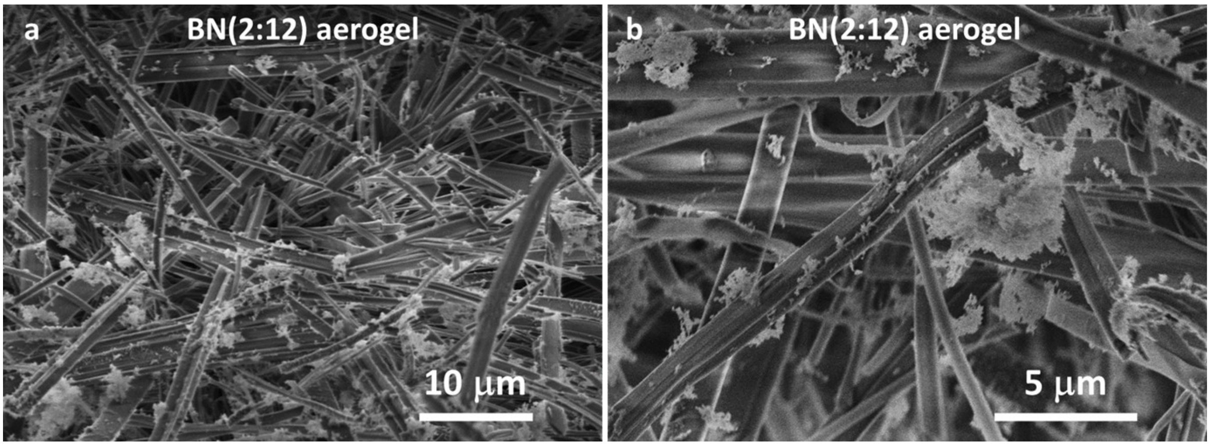

Fig. S9 SEM images of the BN(2:12) aerogel at low (a) and high (b) magnifications.

Fig. S10 Digital photo of the blow torch used for burning BN aerogels.

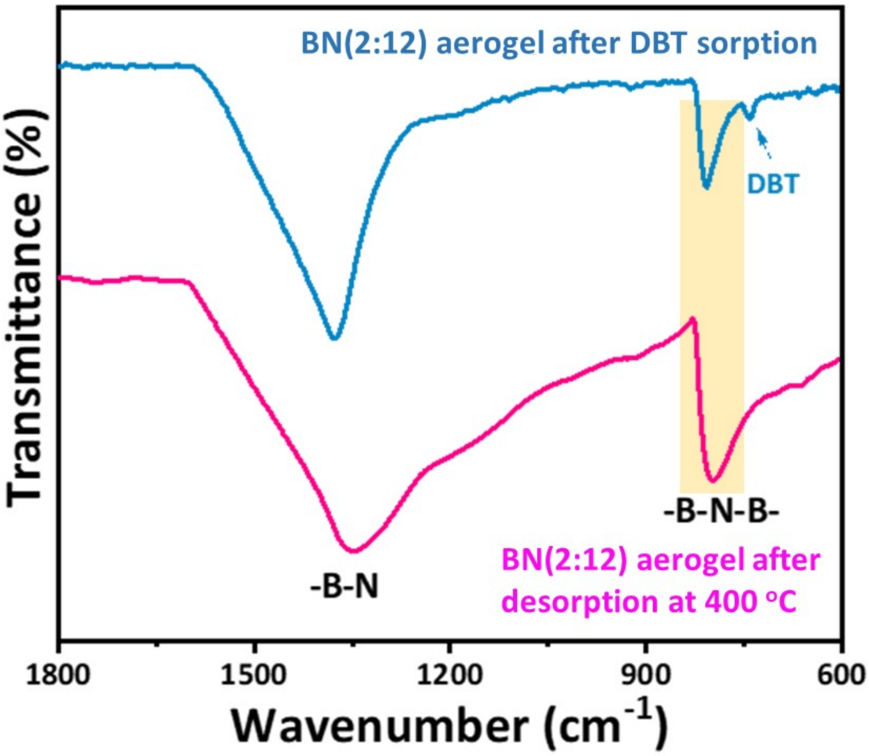

Fig. S11 FT-IR spectra of the BN(2:12) aerogel after DBT adsorption and desorption.